

# FRB Coherent Emission from Decay of Alfvén Waves

Pawan Kumar<sup>\*1</sup> and Željka Bošnjak<sup>2</sup>

<sup>1</sup>*Department of Astronomy, University of Texas at Austin, Austin, TX 78712, USA*

<sup>2</sup>*Faculty of Electrical Engineering and Computing, University of Zagreb, 10000 Zagreb, Croatia*

3 April 2020

## ABSTRACT

We present a model for FRBs where a large amplitude Alfvén wave packet is launched by a disturbance near the surface of a magnetar, and a substantial fraction of the wave energy is converted to coherent radio waves at a distance of a few tens of neutron star radii. The wave amplitude at the magnetar surface should be about  $10^{11}$  G in order to produce a FRB of isotropic luminosity  $10^{44}$  erg  $s^{-1}$ . An electric current along the static magnetic field is required by Alfvén waves with non-zero component of transverse wave-vector. The current is supplied by counter-streaming electron-positron pairs, which have to move at nearly the speed of light at larger radii as the plasma density decreases with distance from the magnetar surface. The counter-streaming pairs are subject to two-stream instability which leads to formation of particle bunches of size of order  $c/\omega_p$ ; where  $\omega_p$  is plasma frequency. A strong electric field develops along the static magnetic field when the wave packet arrives at a radius where electron-positron density is insufficient to supply the current required by the wave. The electric field accelerates particle bunches along the curved magnetic field lines, and that produces the coherent FRB radiation. We provide a number of predictions of this model.

**Key words:** Radiation mechanisms: non-thermal - methods: analytical - stars: magnetars - radio continuum: transients - masers

## 1 INTRODUCTION

It is firmly established that at least a few milli-second duration, very bright, radio signals that have been detected between about 400 MHz and 7 GHz (known as Fast Radio Bursts or FRBs) are coming from a distance of about a Gpc or more, eg. Lorimer et al. 2007; Thornton et al. 2013; Spitler et al. 2014; Petroff et al. 2016; Bannister et al. 2017; Law et al. 2017; Chatterjee et al. 2017; Marcote et al. 2017; Tendulkar et al. 2017; Gajjar et al. 2018; Michilli et al. 2018; Farah et al. 2018; Shannon et al. 2018; Oslowski et al. 2019; Kocz et al. 2019; Bannister et al. 2019; CHIME Collaboration 2019a and 2019b; Ravi 2019a, 2019b; Ravi et al. 2019.

Many mechanisms have been suggested for the generation of high luminosity coherent radio waves from Fast Radio Bursts (FRBs), eg. Katz (2014, 2016), Murase et al. (2016; 2017), Kumar et al. (2017), Metzger et al. (2017), Zhang (2017), Beloborodov (2017), Cordes (2017), Ghisellini & Locatelli (2018), Lu & Kumar (2018), Metzger et al. (2019), Thompson (2019), Wang & Lai (2019), Wang et al. (2019); for a recent review see Katz (2018). Many of these models are severely constrained because of large optical depth for induced Compton scatterings, and radiative acceleration of particles in the vicinity of the source. These models, when they can be made to work, require fine tuning of parameters or very low efficiency for producing radio waves.

The main components of the scenario we explore in this work are

described in Figure 1. A high amplitude Alfvén wave,  $B/B_0 \sim 10^{-4}$ , is launched from the surface of a neutron star (NS) endowed with a strong magnetic field ( $B_0 \gtrsim 10^{15}$  G). Alfvén waves have a non-zero electric current along the magnetic field lines unless the wave vector is exactly parallel to the field line. The current is carried by electrons and positrons moving in opposite directions. This counter-streaming motion of  $e^\pm$  is subject to two-stream instability, which leads to formation of roughly charge neutral particle clumps. As the plasma density decreases with distance from the NS surface, the particle velocity increases in order to carry the current density required by the Alfvén wave. When the plasma density at some height in the NS magnetosphere falls below a critical value, the plasma is unable to support the current even if  $e^\pm$  move at the speed of light. A strong time-dependent electric field then develops, and the displacement current associated with the field makes up for the deficit in plasma current density. The electric field has a component along the static magnetic field just as the plasma current does. This electric field forces electrons and positrons in the clump to move at a high Lorentz factor along magnetic field lines in opposite directions. The coherent curvature radiation produced by these clumps is observed as the FRB signal.

In the next section we describe the basic properties of Alfvén wave propagation through a stratified medium, the development of a strong electric field when the wave becomes charge starved, formation and acceleration of particle clumps. The emission of coherent radiation and predictions of the model are discussed in §3. The main results and limitations of this investigation are summarized in §4.

\* E-mail: pk@astro.as.utexas.edu, zmbosnjak@gmail.com

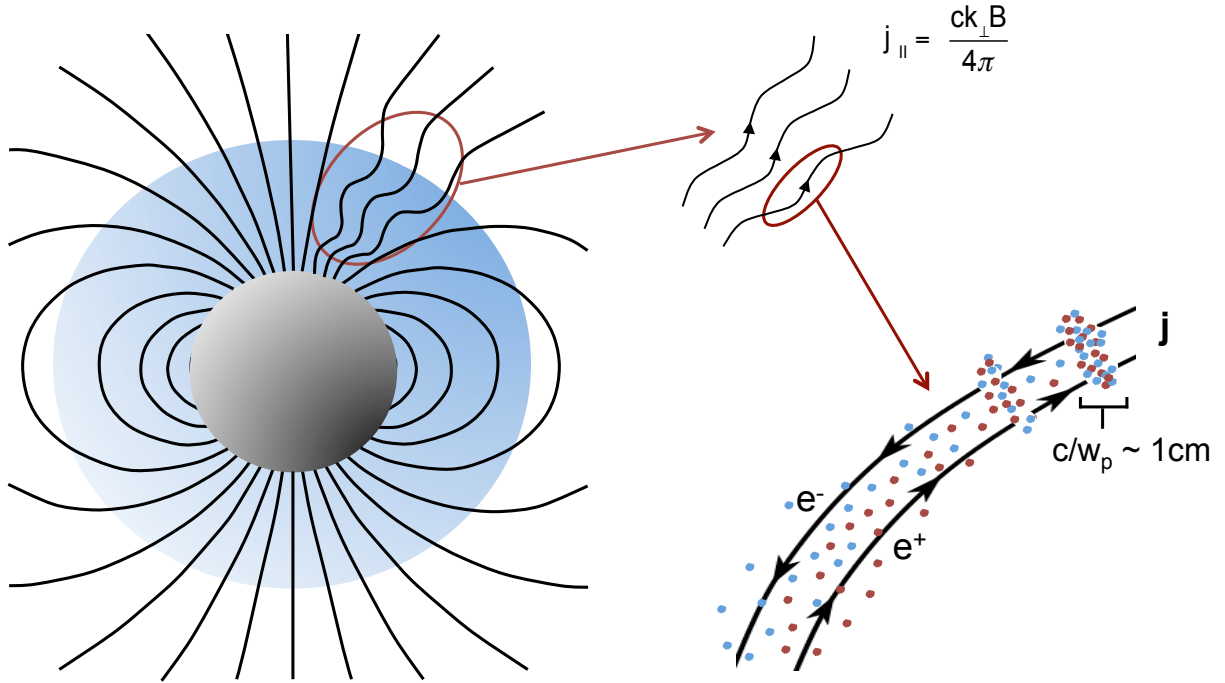


**Figure 1.** This figure provides a schematic overview of the scenario described in this work. A large amplitude Alfvén wave, with magnetic field perturbation of  $B \sim 10^{11}$  G, is produced by some disturbance in the magnetic pole region at the surface of a magnetar (the left-center sketch). As the wave travels to larger radius, outside the shaded region, it becomes charge starved, i.e.  $e^\pm$  density falls below a threshold value of order  $10^{13} (B_{11}/R_7^2) \text{ cm}^{-3}$ , and a strong electric field with a non-zero component along the static magnetic field develops. The Alfvén wave packet has a non-zero current,  $j_\parallel$ , associated with it that is parallel to the large scale static magnetic field (right, top panel). The current is carried by counter-streaming  $e^\pm$  pairs, which is subject to the 2-stream instability and that causes formation of particle clumps of radial width  $\sim c/w_p \sim 1 \text{ cm}$  (right, bottom part of the sketch). When these clumps enter the charge starvation region, they are accelerated by the electric field to Lorentz factor of  $10^3$ . Clumps of particles moving along the curved magnetic field lines produce powerful coherent curvature radiation in the radio band. We find the efficiency of converting Alfvén wave energy to FRB radiation is of order unity.

## 2 ALFVÉN WAVES DISSIPATION AND COHERENT RADIO EMISSION

The process by which Alfvén waves might be generated at the surface of a neutron star (NS) is not well understood. It is possible that these waves are generated by sudden crustal motion, crustal-quake or emergence of magnetic flux tubes from below the surface of a NS. We assume, as have previous work on this subject e.g. Blaes et al. 1989, that Alfvén waves are launched by some mechanism close to the surface of a NS and study their propagation and eventual decay to radio waves.

We describe a few basic properties of Alfvén waves and their propagation in an inhomogeneous medium in the next sub-section, which are needed for this work. Charge starvation of Alfvén waves, generation of electric fields, and particle acceleration are presented in §2.2. Particle bunching due to two-stream instability associated with the Alfvén wave current, and acceleration of bunches are discussed in §2.3.

### 2.1 Alfvén waves

An Alfvén wave-packet launched at the surface of a NS with amplitude  $B$  has isotropic equivalent of luminosity  $L_{aw} = B^2 R_{ns}^2 c \sim 3 \times 10^{44} B_{11}^2 \text{ erg s}^{-1}$ . Therefore, close to the NS  $B \gtrsim 10^{11}$  G is required in order for the Alfvén wave to produce GHz EM waves at the typical FRB luminosity of  $\sim 10^{44} \text{ erg s}^{-1}$  with an efficiency of order

unity (see §3). If the NS has magnetar strength magnetic field, i.e.  $B_0 \sim 10^{15}$  G, then Alfvén waves at the NS surface have dimensionless amplitude  $B/B_0 \sim 10^{-4}$ , and they can be treated as linear perturbation in spite of their enormous luminosity.

We first consider Alfvén waves in a uniform magnetic field using linear perturbation analysis, and subsequently generalize the discussion to an arbitrary magnetic field geometry. The physics of Alfvén waves propagation in a uniform field is straightforward, which can be found in any introductory plasma/MHD text book such as Kulsrud (2005). We include a brief derivation of basic properties of Alfvén waves to establish the notation and to emphasize one particular feature which is that these waves in general have a non-zero current parallel to the static magnetic field. This is one of the key properties we exploit for their dissipation and that leads to generation of coherent curvature radiation.

The uniform magnetic field of magnitude  $B_0$  is taken to be along  $\hat{\mathbf{z}}$ . The perturbation to the field is  $B\hat{\mathbf{x}}$ , and  $B \propto \exp(i\mathbf{r} \cdot \mathbf{k}_{aw} - i\omega_{aw}t)$ ; where the wave-vector  $\mathbf{k}_{aw}$  is in some arbitrary direction. The linearized flux freezing, fluid momentum, and induction equations are

$$\mathbf{E}_\perp = -\frac{\mathbf{v}}{c} \times \mathbf{B}_0, \quad \frac{\partial \rho_e \mathbf{v}}{\partial t} = \frac{\mathbf{B}_0 \cdot \nabla \mathbf{B}}{4\pi}, \quad \nabla \times (\mathbf{v} \times \mathbf{B}_0) = \frac{\partial \mathbf{B}}{\partial t}, \quad (1)$$

where  $\rho_e = \rho_0 + B_0^2/(4\pi c^2)$ , and  $\rho_0$  is the plasma density. These equations can be combined to obtain relationships between  $\mathbf{v}$ ,  $\mathbf{E}_\perp$  &

$\mathbf{B}$ , and the Alfvén wave dispersion relation

$$\frac{\mathbf{v}_\perp}{c} = -\frac{\mathbf{B}}{B_0}, \quad \mathbf{E}_\perp = \mathbf{B} \times \hat{\mathbf{B}}_0, \quad (\mathbf{k}_{\text{aw}} \cdot \hat{\mathbf{B}}_0)^2 V_A^2 = \omega_{\text{aw}}^2, \quad (2)$$

here  $\mathbf{v}_\perp$  is fluid velocity vector perpendicular to the static magnetic field, and  $V_A^2 = c^2 B_0^2 / (4\pi\rho_0 c^2 + B_0^2)$  is very close to  $c^2$  in NS magnetosphere. The first part of equation (2) shows that particles move with the magnetic field in the transverse direction like beads on a wire. In other words, particles stay in the ground state of Landau level all the time and their non-zero transverse velocity is simply to keep up with the perturbed magnetic field lines of the Alfvén wave to which they are locked.

The current associated with the wave can be calculated using the linearized Ampere's equation

$$ic\mathbf{k}_{\text{aw}} \times \mathbf{B} = 4\pi\mathbf{j} - i\omega_{\text{aw}}(\mathbf{E}_\perp + \mathbf{E}_d) \quad (3)$$

where we have explicitly decomposed the electric field as sum of the  $\mathbf{v} \times \mathbf{B}_0$  field given by equation (1), and a field  $\mathbf{E}_d$  which provides displacement current. Making use of equation (2) to eliminate  $\mathbf{E}_\perp$  in terms of  $\mathbf{B}$  simplifies the above equation

$$ic\mathbf{k}_{\text{aw}\perp} \times \mathbf{B} = 4\pi\mathbf{j} - i\omega_{\text{aw}}\mathbf{E}_d, \quad (4)$$

where  $\mathbf{k}_{\text{aw}\perp}$  is the component of  $\mathbf{k}_{\text{aw}}$  perpendicular to the static field  $\mathbf{B}_0$  and the perturbed field  $\mathbf{B}$ , i.e.  $k_{\text{aw}\perp} = \mathbf{k}_{\text{aw}} \cdot (\hat{\mathbf{B}}_0 \times \hat{\mathbf{B}})$ . The left side of the equation drives the system to have non-zero current along  $\hat{\mathbf{B}}_0$ , and possibly a non-zero  $\mathbf{E}_d$ , provided that  $\mathbf{k}_{\text{aw}}$  does not lie in the  $\mathbf{B}_0$ - $\mathbf{B}$  plane. The condition for a non-zero  $E_d$  can be obtained by defining a critical plasma density

$$n_c \equiv \frac{k_{\text{aw}\perp} B}{8\pi q} = (10^{16} \text{ cm}^{-3}) \frac{B_{11}}{\lambda_{\text{aw}\perp,4}}, \quad (5)$$

in terms of which equation (4) can be recast in the following form

$$\frac{\omega_{\text{aw}} \mathbf{E}_d}{8\pi q c} = in(\mathbf{v}_+ - \mathbf{v}_-) / 2c - n_c \hat{\mathbf{B}}_0 \quad (6)$$

where  $\mathbf{v}_+$  ( $\mathbf{v}_-$ ) is the velocity of positrons (electrons), and  $n$  is the plasma density at radius  $R$ . As long as  $n > n_c$ , the plasma has the ability to supply the current needed by the Alfvén wave with  $\mathbf{k}_{\text{aw}\perp} \times \mathbf{B} \neq 0$ . In this case,  $\mathbf{E}_d = 0$  and  $|v_\pm|/c = n_c/n$ . However, when  $n(R) < n_c(R)$ , it is the displacement current,  $\partial \mathbf{E}_d / \partial t$ , along  $\hat{\mathbf{B}}_0$  that must support Alfvén wave's non-zero curl of  $\mathbf{B}$ ; this is defined as the charge starvation region. The electric field in the charge starvation zone, in the limit of vanishingly small plasma density, is

$$\hat{\mathbf{B}}_0 \cdot \mathbf{E}_d = -\frac{8\pi q c n_c}{\omega_{\text{aw}}} = -\frac{k_{\text{aw}\perp}}{k_{\text{aw}\parallel}} B. \quad (7)$$

The critical density is zero for  $k_{\text{aw}\perp} = 0$  (eq. 5). However, for an Alfvén wave packet launched from a region of finite size, it is impossible that  $k_{\text{aw}\perp} = 0$  everywhere. The transverse size of the region from which the Alfvén wave is launched cannot be larger than NS radius ( $\sim 10^6$  cm), and is likely of order the size of polar cap region ( $\ell_{pc}$ ) of open field lines that extend outside the light-cylinder. Thus, we expect  $\lambda_{\text{aw}\perp} \sim \ell_{pc}$ . It is easy to show that for a NS with spin velocity of  $\Omega_{ns}$ , the size of the polar cap is  $\ell_{pc} \sim (R_{ns}^3 \Omega_{ns} / c)^{1/2} \sim 5 \times 10^3 \Omega_{ns}^{1/2}$  cm. If the Alfvén wave frequency is  $10^9$  Hz, then  $k_{\text{aw}\perp} / k_{\text{aw}\parallel} \sim 30$  at the surface of the NS.

The Alfvén wave-packet travels along magnetic field lines and its amplitude decreases as the field lines diverge or flare up with distance;  $B \propto R^{-3/2}$  to conserve luminosity<sup>1</sup>. Therefore, the critical density

<sup>1</sup> The magnetic field decreases with distance as  $\sim R^{-3}$ , and so  $B/B_0 \propto R^{3/2}$ , i.e. the wave becomes increasingly more nonlinear with distance from its launching site.

$n_c \propto R^{-3/2} k_{\text{aw}\perp}$  (see eq. 5). The component of Alfvén wave-vector along  $\hat{\mathbf{B}}_0$ ,  $k_{\text{aw}\parallel}$ , is conserved as it is equal to  $\omega_{\text{aw}}/c$ . The wave-vector component perpendicular to the magnetic field  $k_{\text{aw}\perp}$ , however, decreases with  $R$ , approximately as  $R^{-3/2}$ , since the transverse size of the wave packet increases as  $R^{3/2}$  due to the spreading of magnetic field lines. The precise behavior of  $\mathbf{k}$  with distance is determined by solving the following Eikonal equations, e.g. (Weinberg, 1962)

$$\frac{d\mathbf{x}}{dt} = c\hat{\mathbf{B}}_0, \quad \frac{dk_{\text{aw}}^i}{dt} = -c \sum_{j=1}^3 k_{\text{aw}}^j \frac{\partial \hat{B}_{0j}}{\partial x_i}. \quad (8)$$

The solution of this equation is shown in Fig. 2 for a dipole magnetic field, and it is clear that the component of  $\mathbf{k}_{\text{aw}}$  transverse to the local magnetic field direction does indeed decrease approximately as  $R^{-3/2}$ . Therefore,  $k_{\text{aw}\perp} / k_{\text{aw}\parallel} \propto R^{-3/2}$  and it becomes of order unity at the radius where the wave becomes charge starved.

The critical density as a function of  $R$  is given by

$$n_c(R) \equiv \frac{k_{\text{aw}\perp} B}{8\pi q} \approx (10^{16} \text{ cm}^{-3}) \frac{B_{11}}{\lambda_{\text{aw}\perp,4}} \left[ \frac{R_{ns}}{R} \right]^3, \quad (9)$$

where the factor  $B_{11} / \lambda_{\text{aw}\perp,4}$  is evaluated at the NS surface. Since  $n_c \propto R^{-3}$ , the current along  $\hat{\mathbf{B}}_0$  required by the Alfvén wave packet can be supplied by the magnetosphere plasma provided that particle density  $n(R)$  does not decrease faster than  $R^{-3}$ . We address this next.

The particle density in the NS magnetosphere is controlled by the magnetic field and the rotation rate (Goldreich & Julian, 1969). Charge particles with a minimum number density  $n_{GJ}$  (Goldreich-Julian density) fill the magnetosphere. Otherwise, the electric field is so strong as to pull charge particles from NS surface or create  $e^\pm$  spontaneously. The actual particle density is taken to be a factor  $\mathcal{M}$  larger than the minimum required density:

$$n = \mathcal{M} n_{GJ} = \frac{\mathcal{M} \mathbf{B}_0 \cdot \Omega_{ns}}{2\pi q c} \approx \frac{\mathcal{M} B_{ns} \Omega_{ns}}{2\pi q c} \left( \frac{R_{ns}}{R} \right)^3 \approx 10^{13} \text{ cm}^{-3} \mathcal{M} B_{ns,15} \Omega_{ns} \left( \frac{R_{ns}}{R} \right)^3. \quad (10)$$

The value of  $\mathcal{M}$  is highly uncertain and is estimated to be anywhere between a few and  $\sim 10^6$  for pulsars. Therefore, it is possible that  $\mathcal{M}$  is a function of  $R$ , and that  $n = \mathcal{M} n_{GJ} \propto \mathcal{M} R^{-3}$  declines faster than  $R^{-3}$  at some radius.

Comparing the critical density (eq. 5) with the particle density in NS magnetosphere (eq. 10), we find that  $n_c > n$  unless  $\mathcal{M} \gtrsim 10^3$ . So,  $\mathcal{M}$  should be sufficiently large near the Alfvén wave launching site to ensure that wave is not charge starved at birth. As long as this condition is satisfied, the wave-packet will travel to larger radius without becoming charge starved until  $\mathcal{M}$  starts to decrease. If at some radius  $R_c$  the particle density  $n$  falls below  $n_c$  due to the decrease of  $\mathcal{M}$ , then the wave becomes charge starved and a strong electric field with a component parallel to the static magnetic field develops. The radius where the charge starvation sets in is likely not very far away from the NS since  $n_c \gg n_{GJ}$ , so  $\mathcal{M}$  only needs to drop a bit for the wave to enter the charge starvation regime. The development of electric field and particle acceleration when Alfvén waves become charge starved is discussed in the next sub-section.

## 2.2 Charge starvation and particle acceleration

The Alfvén wave-packet encounters decreasing particle density as it propagates out to larger radius. When the ambient medium density approaches the critical density ( $n_c$ ; eq. 5), charge particles begin to move at close to the speed of light to supply the current needed by

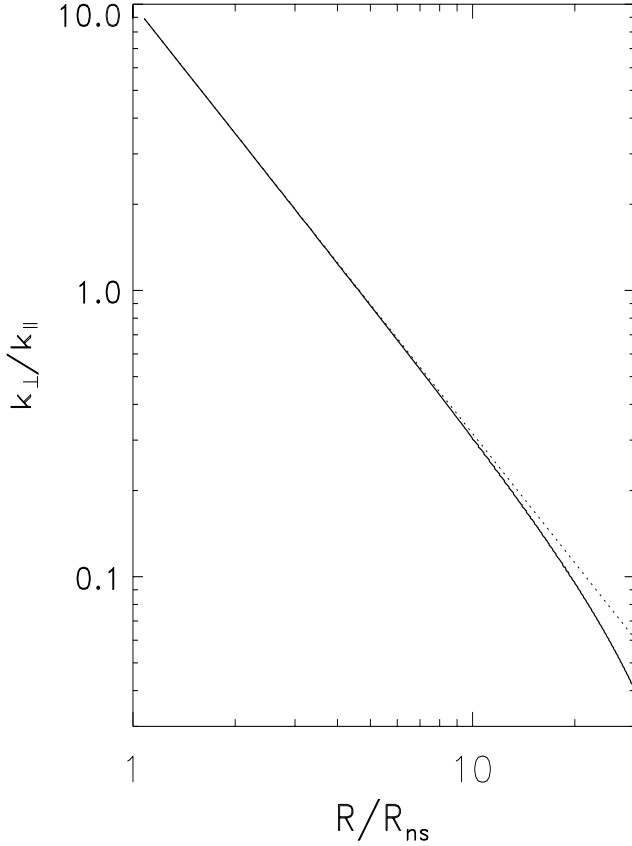


**Figure 2.** Shown here is the component of wave-vector  $\mathbf{k}$  perpendicular to the local magnetic field, i.e.  $\hat{\mathbf{B}}_0 \times \mathbf{k}$ ; the magnetic field is taken to be dipolar. The distance is measured in unit of neutron star radius, and the wave-number is in units of  $\omega_{aw}/c$ ; where  $\omega_{aw}$  is Alfvén wave frequency. Shown also is  $R^{-3/2}$  curve (dotted line) for comparison.

the Alfvén wave. An electric field must develop when  $n$  falls below  $n_c$ , because the plasma cannot supply the current for the Alfvén wave and the deficit is compensated by the displacement current. In other words, the right-hand-side of linearized Amperes equation

$$\frac{\partial \hat{\mathbf{B}}_0 \cdot \mathbf{E}_d}{\partial t} = -4\pi \hat{\mathbf{B}}_0 \cdot \mathbf{j} + ic\mathbf{B} \cdot (\hat{\mathbf{B}}_0 \times \mathbf{k}_{aw\perp}), \quad (11)$$

is non-zero for  $n < n_c$  and that leads to a non-zero  $\hat{\mathbf{B}}_0 \cdot \mathbf{E}_d$ ;  $k_{aw\perp} \equiv \mathbf{k}_{aw} \cdot (\hat{\mathbf{B}}_0 \times \hat{\mathbf{B}})$ . Although, the solution of equation (11) can be quite involved if the density of the medium is a non-smooth function. We will ignore that complication and consider the average electric field component parallel to the static magnetic field which can be written as

$$\hat{\mathbf{B}}_0 \cdot \mathbf{E}_d = E_d \exp(ik_{aw\parallel}\xi - i\omega_{aw}t), \quad (12)$$

where  $\xi$  is distance along a magnetic field line.

The particle motion is restricted along  $\hat{\mathbf{B}}_0$ , because the static magnetic field is strong and particles are stuck in the lowest Landau level. The equation for motion under the influence of the electric field, in the charge starvation region, in this case is

$$\frac{d\gamma\beta}{dt} = \frac{qE_d}{mc} \sin[\omega_{aw}(\xi/c - t)]. \quad (13)$$

Let us define

$$\omega_E = \frac{qE_d}{mc}, \quad a_{aw} = \frac{qE_d}{mc\omega_{aw}}, \quad \phi = \omega_{aw}(\xi/c - t). \quad (14)$$

The equation for particle motion is rewritten in terms of these as

$$(1-\beta) \frac{d\gamma\beta}{d\phi} = -a_{aw} \sin \phi \implies \frac{d\gamma(1-\beta)}{d\phi} = -a_{aw} \sin \phi. \quad (15)$$

The solution of this equation is

$$\gamma(1-\beta) = \gamma_0(1-\beta_0) - a_{aw}(\cos \phi - \cos \phi_0), \quad (16)$$

where  $\phi_0$  and  $\beta_0$  are the initial particle position (phase) and speed;  $\gamma_0(1-\beta_0) \sim 1$ . If  $a_{aw}$  is positive, then for  $0 < \phi_0 < \pi$ , the particle acceleration is along the same direction as the Alfvén wave propagation direction, and the asymptotic value for  $\cos \phi$  is  $\cos \phi_0 + \gamma_0(1-\beta_0)/a_{aw}$ . Since  $a_{aw} = 2 \times 10^{10} E_{d,8} \omega_{aw,5}^{-1}$ , the particle is carried by the wave and stays very nearly at the same wave-phase. This is because the particle is accelerated by the wave to highly relativistic speeds in a time much shorter than the wave period, and the particle moves with the wave at nearly a fixed phase. The difference between particle speed and the wave speed is  $c/(2\gamma^2)$ , which is extremely small for large  $\gamma$ , and that is the reason that the particle stays at roughly the initial phase angle.

Particles of opposite charge, i.e.  $a_{aw} < 0$ , and  $0 < \phi_0 < \pi$ , are accelerated along the direction opposite to the Alfvén wave velocity vector. In the absence of radiative losses, particles are accelerated to Lorentz factor  $\sim |a_{aw}|/2$ . Curvature radiation loss, acting on particles individually, limits the particle LF to  $\sim 10^8 E_{d,8}^{1/4} R_{B,8}^{1/2}$ ; where  $R_B$  is the curvature radius of magnetic field. We will see in the next subsection that  $\gamma \lesssim 10^3$  due to radiation reaction force on particle bunches that radiate coherently.

These particles, i.e. those with  $a_{aw} < 0$  &  $0 < \phi_0 < \pi$ , moving close to the speed of light toward the rear end of the Alfvén wave-packet arrive at a location in about one half wave period where the wave-electric-field direction has reversed, and they are then pulled in the opposite direction. Their dynamics is now described by the  $a_{aw} > 0$  case discussed above. These particles are trapped in a narrow region if  $\gamma \ll a_{aw}$  and dragged with the wave for a distance  $\sim c\gamma^2/\omega_{aw}$ , which is essentially forever for the system of interest to us.

When the Alfvén wave enters the charge starvation region, it drags with it charges of one sign in one-half-wavelength and particles of opposite charge in the adjoining half-wavelength which has electric field of opposite sign. The Coulomb field due to this charge separation is

$$E_{cou} \sim 2\pi^2 qn/k_{aw\parallel}, \quad \text{or} \quad E_{cou} \lesssim \frac{\pi B}{4} \frac{k_{aw\perp}}{k_{aw\parallel}} \lesssim E_d. \quad (17)$$

The inequality follows from  $n < n_c$  and using equations (6) & (5) for  $E_d$  &  $n_c$ . The Coulomb field is smaller than the electric field  $\hat{\mathbf{B}}_0 \cdot \mathbf{E}_d$  associated with the Alfvén wave (eq. 7). The energy stored in the Coulomb field per unit volume is of order, but smaller than, the Alfvén wave energy density. Thus, when the Alfvén waves enter the charge starvation region, a fraction of their energy gets expended to charge separation. The kinetic energy density of particles is much smaller than the Alfvén wave energy density ( $B^2/8\pi$ ), since particle LF is smaller than the maximum value of  $|a_{aw}|/2$  due to the radiation reaction force.

Electrons and positrons are advected by the Alfvén wave at the charge starvation radius  $R_c$ , and the resulting charge depletion in the interior of  $R_c$  causes the starvation front to shift to smaller radius with time.

Particles below  $R_c$  move along  $\hat{\mathbf{B}}_0$  at high speeds to supply the

current for the Alfvén wave. Thus, there is a continuous flux of particles crossing  $R_c$  from below. These particles get accelerated to high LF and advected with the Alfvén wave as a result of the strong electric field<sup>2</sup> in the charge starvation zone. The continuous loss of particles from the interior of  $R_c$  causes the  $e^\pm$  density to decrease with time, and the region which was not charge starved before becomes charge starved. We estimate the speed at which  $R_c$  moves inward.

The current amplitude ( $I_{aw}$ ) associated with the Alfvén wave-packet along  $\hat{\mathbf{B}}_0$  is roughly independent of  $R$ ;  $I_{aw}$  is the integral of current density over the cross-section of the wave-packet. Thus, the number of particles that cross  $R_c$  per unit time, and are subsequently advected by the Alfvén wave is  $\sim I_{aw}/2q$ . The cross-sectional area of the wave packet,  $A_{aw}$ , increases as  $R^3$  as the wave follows the dipole field lines. Therefore,  $dR_c/dt \sim -I_{aw}/(2qnA_{aw})$ . This result can be recast in a slightly more convenient form as  $dR_c/dt \sim -n_c/2n$ ;  $I_{aw}/A_{aw} \sim j$ , and  $j$  can be written in terms of  $n_c$  and  $n$  using equations (4) & (6).

A corollary of this result is that  $e^\pm$  present in the NS magnetosphere are depleted (advected by the wave) on a time of order  $(n/n_c)R_c/c$ , which is a few ms.

Thus far, we have discussed how the Alfvén-current below  $R_c$  supplies a flux of particles into the charge-starvation region where they are quickly accelerated and advected by the wave. We now describe how particles the Alfvén wave-packet encounters at the head of the wave at  $R > R_c$  also get trapped and advected by the wave. Charge particles of one sign – those which experience the force of the field  $\mathbf{E}_d$  in the forward direction – are swept up by the wave front and compressed into a thin sheet of width much smaller than  $\lambda_{aw}$  and forced to move with the wave. Particles of the opposite charge move in the reverse direction, along  $-(\hat{\mathbf{k}}_{aw} \cdot \hat{\mathbf{B}}_0)\hat{\mathbf{B}}_0$ , at speed  $\approx c$  for about half a wavelength and there they start accumulating in a thin sheet; these results follow from equation (16) for  $\gamma$ .

The Coulomb field in the thin sheet increases with time as more charges are swept up by the wave and accumulate in the sheet:

$$E_{cou}(t) \sim \pi q n (R - R_c), \quad \text{for } R > R_c \quad (18)$$

where  $R$  is the location of the wavefront at time  $t$ . The Coulomb field strength exceeds the wave-field  $E_d$  for  $(R - R_c) \gtrsim \lambda_{aw}$ , and at that point the sheet starts spreading in the longitudinal direction at close to the speed of light. Since the Coulomb fields at the front and the back sides of the sheet do not decrease as the width of the sheet increases, the spreading continues until the sheet thickness becomes  $\sim \lambda_{aw}/2$ . Particles in the sheet now overlap with particles of opposite charge in the adjoining half-wavelength of the Alfvén packet thereby partially shielding  $E_{cou}$ .

The physics of the system is that charge particles of one sign swept up at the front of the Alfvén wave-packet, within  $\lambda_{aw}$  of  $R_c$ , accumulate in a thin sheet near the leading front. The sheet starts to spread longitudinally, after about one wave period, when the Coulomb field in the sheet exceeds the wave-electric-field. Thereafter, particles swept up at the front of the wave form an alternating positive and negative charge particle streams, separated by half a wavelength, that move toward the rear end of the wave-packet. This charge particle stream partially neutralizes the charge separation discussed previously where

<sup>2</sup> The current density,  $\mathbf{j}$ , and the electric field  $\mathbf{E}_d$  (which provides the displacement current) point in the same direction as per the Ampere's law. Thus, charge particles of the sign that cross  $R_c$  encounter electric field there that is pointing in a direction such that these particles are accelerated in the forward direction, i.e. to larger  $R$ , and not forced back to  $R < R_c$ . In other words, the electric field direction in the charge starvation region is such that it continuously removes charge particles from the interior.

the Alfvén wave packet advects particles with it from the boundary of charge starvation region at radius  $R_c$ .

We close this sub-section by summarizing the main results.

1. The Alfvén wave-packet moving away from the surface of the NS becomes charge starved at some radius  $R_c$  when the particle density falls below a critical value and the plasma is unable to carry the current required by the wave. An electric field develops at  $R > R_c$ , which has a non-zero component along the magnetic field; at  $R > R_c$  the displacement current makes up for the deficit in plasma current.
2. Charge particles are separated at  $R_c(t)$  by the electric field, and advected by different segments of the Alfvén wave-packet, roughly half wavelength apart, where the electric force on them is in the forward direction (the direction of the wave motion). The charge starvation radius moves closer to the NS with time as particle density in the neighborhood of  $R_c$  decreases.
3. Charge particles of one sign swept up at the head of the Alfvén packet are compressed into a thin sheet. When the coulomb force in the sheet becomes too large to confine particles, they spread longitudinally to the rear of the wave-packet. Streams of particles of different charges move at different speeds toward the rear of the wave, and they are subject to two-stream instability that causes particles to form clumps.

Clumps of particles advected by the Alfvén wave move along the curved magnetic field lines and produce coherent curvature radiation that is discussed in section 3.

### 2.3 Formation and acceleration of particle clumps

Alfvén wave packets of finite size in the direction perpendicular to the magnetic field  $\mathbf{B}_0$  must have a non-zero component of the wave-vector transverse to the field. Therefore, the wave packet has a non-zero current along the magnetic field lines as was shown in §2.1. Electrons and positrons that carry this current are subject to two stream instability, and that leads to formation of particle clumps. The particle clumps are accelerated by the electric field in the charge starvation region. We estimate clump LF in this sub-section. The clumps moving along curved magnetic field lines produce coherent curvature radiation that is responsible for the FRB signal (§3).

Growth rate of the 2-stream instability, for  $e^\pm$  moving at sub-relativistic speeds, is obtained by solving the following equation (eg. Chen, 1974)

$$\frac{\omega_p^2}{\omega^2} + \frac{\omega_p^2}{(\omega - kv)^2} = 1, \quad (19)$$

where  $v$  is the relative speed between  $e^\pm$ s,  $(\omega, k)$  are frequency and wavenumber for the 2-stream instability, and

$$\omega_p = \left[ \frac{4\pi q^2 n}{m} \right]^{1/2} \quad (20)$$

is the plasma frequency. The imaginary part of  $\omega$  gives the growth rate of the instability. The growth rate for  $k \ll \omega_p/v$  is  $kv/2$ . The growth rate peaks at  $k \sim 1.5\omega_p/v$  where its value is  $\sim \omega_p/2$ . The instability leads to formation of particle clumps of longitudinal size  $\sim \pi v/\omega_p$ . The particle density at the charge starvation radius,  $R_c$ , is  $\sim n_c$  (eq. 9), and therefore the longitudinal size of a typical clump is

$$\ell_{\parallel} \sim c \left( \frac{\pi m}{4q^2 n_c} \right)^{1/2} \sim 0.5 \text{ cm} \left[ \frac{\lambda_4^{aw}(R_{ns})}{B_{11}(R_{ns})} \right]^{1/2} \left[ \frac{R_c}{10R_{ns}} \right]^{3/2}, \quad (21)$$

where  $\lambda^{aw\perp} \equiv 2\pi/k_{aw\perp}$ , and  $k_{aw\perp}$  is the transverse component of Alfvén wave-vector.

Clumps form on the plasma time scale, which is much smaller than the period of the Alfvén wave; the timescale for the former, for the system we are considering, is  $\sim 0.1$  nano-second whereas the latter is longer than  $1 \mu\text{s}$ . These results apply to mildly relativistic velocity as well, and for the highly relativistic motion introduction of the usual Lorentz factor gives the correct growth rate.

The electric field associated with Alfvén waves in the charge starvation region is expected to be  $\sim 10^8$  esu for  $k_{aw\perp}/k_{aw\parallel} \sim 0.1$  (eq. 7 & fig. 2), and even in the transition region before the charge starvation radius the field strength is likely of order  $\gtrsim 10^5$  esu. Electrons and positrons are accelerated to LF of  $10^2$  when traveling a distance of 17 micro-meter in an  $10^8$  esu field. Were it not for the radiation reaction (RR) forces, these particles would attain  $\gamma \sim 10^{10}$  if the field extends to 1 km. Charge particles moving along curved magnetic field lines produce curvature radiation and the back reaction of this radiation limits the particle LF. The power emitted by an electron moving with LF  $\gamma$  along a magnetic field line of curvature radius  $R_B$  is

$$p_c = \frac{2q^2\gamma^4 c}{3R_B^2}. \quad (22)$$

The characteristic frequency of curvature radiation depends on  $\gamma$  &  $R_B$ , and is given by

$$\nu \approx \frac{c\gamma^3}{2\pi R_B}, \quad \text{or} \quad \gamma \approx (2\pi\nu R_B/c)^{1/3} \approx 590 (R_{B,9} \nu_9)^{1/3}. \quad (23)$$

The curvature radius of a dipole magnetic field line at location  $(R, \theta)$  is

$$R_B(R, \theta) \approx 0.8 R/\theta, \quad (24)$$

where the polar angle  $\theta$  is measured wrt to the magnetic axis.

The back reaction of the curvature-radiation acting on particles individually limits their LF to  $\sim 10^8 E_{d,8}^{1/4} R_{B,8}^{1/2}$ ; this is obtained by equating the rate of work done by the electric field with the rate of loss of energy to radiation<sup>3</sup>.

However, radiative reaction forces do not act on particles individually when the wavelength of the curvature radiation is larger than the inter-particle distance. The calculation of collective RR force on a particle bunch is a challenging problem. In fact, RR force calculation on a single particle is already a hard problem. The Abraham-Lorentz prescription for RR force for a non-relativistic particle (Landau & Lifshitz, 1971), and Dirac's generalization to particles with relativistic speed (Dirac, 1938) suffer from pathological properties such as particle acceleration in advance of the force. A number of fixes have been suggested to make RR force formulae respect causality, however, they are ad hoc patches and not derived from first principles considerations.

Our best hope going forward, therefore, is to use general principles of energy conservation and causality to guide the estimate of Lorentz factor of a particle bunch that is radiating coherently and is subject to collective RR forces. The LF is obtained by balancing the rate of energy supply to a particle by the electric field and the rate of loss of energy to radiation as a member of a large group of particles radiating in phase.

Let us consider that the electric field that accelerates particles is turned on linearly with time, which is reasonable considering that the

<sup>3</sup> This result is unphysical at high plasma densities when the kinetic energy density in particle with this LF exceeds the energy density of electric field. The electric field is shorted out by rapid redistribution of  $e^\pm$  on the plasma timescale.

displacement current  $(\partial \mathbf{E}_d/\partial t)$  is compensating for the deficit in the plasma current,

$$E(t) = \dot{E}t, \quad \dot{E} = \frac{E_0}{t_0} \quad \text{for } t < t_0. \quad (25)$$

The field  $E(t)$  is the electric field  $E_d$  of §2.2 along the worldline of a particle. The energy equation for the charge particle before the RR force becomes important is

$$\frac{dm\gamma c^2}{dt} = q\dot{E}t, \quad (26)$$

which can be rewritten as

$$\frac{d\gamma^2}{dt} = \frac{2q\dot{E}(\gamma\beta)t}{mc} \quad \text{or} \quad \frac{d(\gamma^2 - 1)^{1/2}}{dt} = \frac{q\dot{E}t}{mc}. \quad (27)$$

The solution of this equation is

$$[\gamma^2(t) - 1]^{1/2} = \frac{q\dot{E}t^2}{2mc}. \quad (28)$$

Or

$$\gamma(t) \approx 2(t/t_a)^2 \quad \text{for } t_a < t < t_0, \quad (29)$$

where

$$t_a = \left[ \frac{12^{1/2} mc}{q\dot{E}} \right]^{1/2} = (4.4 \times 10^{-10} \text{ s}) \frac{t_{0,-7}^{1/2}}{E_{0,5}^{1/2}}. \quad (30)$$

The radiation reaction force acts on a group of particles collectively that are radiating in phase. It is convenient to define a coherent volume,  $V_{coh}$ , such that

$$N_{coh} \equiv n(R) V_{coh} \quad (31)$$

is the number of particles that radiate in phase, and are subject to the collective RR force;  $n$  is the plasma density. The coherent volume depends on  $\gamma$ ,  $\lambda$  (wavelength of radiation), the density fluctuation spectrum of the plasma along the photon propagation direction  $[\tilde{n}(k)]$  or typical clump size ( $\ell_{\parallel}$ ), and time  $t$  which sets an upper limit on  $V_{coh}$  from causality considerations. At time  $t$  – measured from the moment when the electric field is turned on – the coherent volume cannot be larger than  $(ct)^3$ .

Curvature radiation from different electrons or positrons moving with LF  $\gamma$  can add coherently provided that their velocity and acceleration vectors are nearly parallel to within an angle  $\gamma^{-1}$  and they all lie inside  $V_{coh}$ . If the emission region is at radius  $R$ , and particles are moving along the dipole magnetic field lines, then these conditions require the transverse size of the coherent region,  $\mathcal{L}_{\perp}$ , to be no larger than  $R/\gamma$ . Combining this with the causality condition leads to

$$\mathcal{L}_{\perp} \approx \min\{ct, R/\gamma, w_{aw}\}, \quad (32)$$

where  $w_{aw}$  is the transverse width of the Alfvén wave packet at  $R$  or the width of the region where particles are accelerated. We will assume for the rest of this work that  $w_{aw}$  is larger than the other two scales; it is straightforward to modify all the relevant formulae if  $\mathcal{L}_{\perp} = w_{aw}$ .

The size of the coherent region in the longitudinal direction (along particle velocity vector),  $\mathcal{L}_{\parallel}$ , is a more complicated entity which depends on all the variables of the system mentioned above, viz.  $t$ ,  $\lambda$ ,  $\gamma$ ,  $\tilde{n}$ ,  $\ell_{\parallel}$ . The dynamical time in the rest frame of a clump at radius  $R$  that is moving with LF  $\gamma$  is  $R/c\gamma$ , and the size of the region in causal contact in this frame is  $R/\gamma$ . Therefore, the maximum size of causally connected region in the lab frame is  $R/\gamma^2$ . Let us consider that a clump has been accelerated to  $\gamma$  by an electric field turned on

time  $t$  ago. If  $ct$  is smaller than the characteristic wavelength of curvature photons<sup>4</sup>, then causality suggests that  $\mathcal{L}_{\parallel} \sim \min\{ct, R/\gamma^2\}$ .

Curvature radiation from particles separated by  $\lambda/2$  along the photon propagation direction nearly cancels when  $ct \gg \lambda$ . The contribution to the luminosity from a region of longitudinal size  $\lambda$  is non-zero when  $\tilde{n}(2\pi/\lambda) \neq 0$ . Let us consider that the medium is clumpy and the typical clump size is  $\ell_{\parallel}$  in the longitudinal direction. For  $\lambda > \ell_{\parallel}$ , the net emission from a region of size  $\lambda$  depends on the difference between the number of particles in the adjacent two half-wavelengths, which is roughly proportional to  $(\lambda/\ell_{\parallel})^{1/2}$ . Therefore,  $\mathcal{L}_{\parallel} \sim \ell_{\parallel}$  in this case as different particle clumps are randomly placed within a wavelength and the electric fields of radiation from them have random relative phases. Similar considerations for  $\lambda < \ell_{\parallel}$  lead to  $\mathcal{L}_{\parallel} \sim |\tilde{n}(k)|/n$  with  $k \sim \pi/\lambda$ . Results for these different cases are summarized in the following equation

$$\mathcal{L}_{\parallel} \sim \begin{cases} \min\{ct, R/\gamma^2\} & ct < \lambda \ \& \ \ell_{\parallel} \\ \ell_{\parallel} & ct > \lambda > \ell_{\parallel} \\ |\tilde{n}(\pi/\lambda)|/n & ct > \lambda < \ell_{\parallel} \end{cases} \quad (33)$$

The number of particles that experience collective radiation-reaction force can be rewritten in terms of  $\mathcal{L}_{\parallel}$  &  $\mathcal{L}_{\perp}$  as

$$N_{coh} = n V_{coh} \sim n \mathcal{L}_{\parallel} \mathcal{L}_{\perp}^2. \quad (34)$$

The acceleration of a clump passes through a few different stages of the nine cases covered by equations (32) and (33) depending on various parameters of the system.

Initially, the coherent volume grows with time as,  $V_{coh} \sim n(ct)^3$  [eqs. 32] & [33]. Balancing the rate of work done by the electric field on particles within  $V_{coh}$  with the rate of loss of energy to curvature radiation by these particles collectively, we find

$$qE(t)c \approx p_c N_{coh} \implies \gamma \approx \left[ \frac{3\dot{E}R_B^2}{2qnc^3t^2} \right]^{1/4}. \quad (35)$$

The time  $t_{rr}$  when the RR force becomes important is when  $\gamma$  given by equations (28) and (35) are roughly equal, i.e.

$$\frac{q\dot{E}t^2}{2mc} \sim \left[ \frac{3\dot{E}R_B^2}{2qnc^3t^2} \right]^{1/4}, \quad (36)$$

or

$$t_{rr} \sim \left[ \frac{24R_B^2 m^4 c}{q^5 \dot{E}^3 n} \right]^{1/10} \sim (5 \times 10^{-9} \text{s}) R_{B,8}^{1/5} \dot{E}_{12}^{-3/10} n_{13}^{-1/10}. \quad (37)$$

The LF for  $t < t_{rr}$  is given by equation (28) and for  $t > t_{rr}$  by equation (35). The particle LF and the wavelength of the curvature radiation at time  $t_{rr}$  are

$$\gamma(t_{rr}) \sim 300 (R_{B,8} \dot{E}_{12})^{2/5} n_{13}^{-1/5}, \quad \lambda(t_{rr}) \sim (20 \text{ cm}) R_{B,8}^{-1/5} \dot{E}_{12}^{-6/5} n_{13}^{3/5}. \quad (38)$$

If the parameters are such that  $ct_{rr} < \lambda$ , then with time this inequality grows only bigger (as  $\lambda \propto \gamma^{-3} \propto t^{3/2}$ ) and the evolution of  $\gamma$  continues to be described by equation (35) for a while. However, for the parameters relevant for FRBs,  $ct_{rr} > \lambda$ ,  $\lambda \gtrsim \ell_{\parallel}$ , and  $ct_{rr} < R/\gamma$ . Therefore, the coherent volume for the calculation of RR force should

<sup>4</sup> Technically it is incorrect to talk about  $\lambda > ct$ , as photons of wavelength  $\lambda$  can not be produced in time less than  $\lambda/c$ . However, what we are quantifying here is the longitudinal size of the region where all particles (of the same charge) are radiating in phase, and that size cannot exceed  $ct$ , i.e.  $\mathcal{L}_{\parallel} \lesssim ct$ .

be  $V_{coh} \sim \ell_{\parallel}(ct)^2$  instead of  $(ct)^3$ . The evolution of clump LF in this case is provided by the following equation:

$$q\dot{E}t c \approx p_c n V_{coh} \implies \gamma(t) \approx \left[ \frac{3\dot{E}R_B^2}{2qnc^2 t \ell_{\parallel}} \right]^{1/4},$$

$$\text{or } \gamma(t) \sim 1.4 \times 10^3 \left[ \frac{\dot{E}_{12} R_{B,9}^2}{n_{13} t_{-7} \ell_{\parallel}} \right]^{1/4}. \quad (39)$$

The time when the collective RR force becomes important and starts to dominate the clump dynamics is obtained from the following equation

$$\frac{q\dot{E}t^2}{2mc} \sim \left[ \frac{3\dot{E}R_B^2}{2qnc^2 t \ell_{\parallel}} \right]^{1/4} \implies t_{rr} \sim \left[ \frac{24c^2 m^4 R_B^2}{q^5 n \dot{E}^3 \ell_{\parallel}} \right]^{1/9},$$

$$\text{or } t_{rr} \sim (9 \times 10^{-9} \text{s}) R_{B,8}^{2/9} n_{13}^{-1/9} \dot{E}_{12}^{-1/3} \ell_{\parallel}^{-1/9}. \quad (40)$$

The LF decreases with time as  $t^{-1/4}$  for  $t > t_{rr}$  if the electric field increases linearly with time; the decrease is slower if  $\dot{E}$  rises with time, and for  $t < t_{rr}$  the LF is given approximately by equation (28). The LF of the particle clump at  $t_{rr}$  is

$$\gamma(t_{rr}) \sim \frac{q\dot{E}t_{rr}^2}{2mc} \sim 700 \frac{\dot{E}_{12}^{1/3} R_{B,8}^{4/9}}{(n_{13} \ell_{\parallel})^{2/9}}, \quad (41)$$

and the wavelength of curvature photons at this time is

$$\lambda(t_{rr}) \approx \frac{2\pi R_B}{\gamma^3(t_{rr})} \sim (1.1 \text{ cm}) \dot{E}_{12}^{-1} R_{B,8}^{-1/3} (n_{13} \ell_{\parallel})^{2/3}. \quad (42)$$

Thus,  $\lambda(t_{rr}) < ct_{rr}$ , and the clump LF was calculated with  $V_{coh}$  in the correct regime (eq. 33). Since,  $\gamma \propto (\dot{E}/t)^{1/4}$  and  $\lambda \propto \gamma^{-3} \propto (t/\dot{E})^{3/4}$ , for the entire visible worldline of the clump  $\lambda/ct < 1$ .

At the time,  $t_{rr}$ , when the RR force begins to dominate the dynamics,  $R/\gamma > ct_{rr}$  (for  $R \gtrsim 10^6 \text{ cm}$ , see eq. 40) and this ordering is preserved up to time  $\sim (3 \mu\text{s}) R_{B,8}^{4/3} (n_{13} \ell_{\parallel})^{1/3} / (\dot{E}_{12}^{1/3} R_{B,8}^{2/3})$ . The radiation we observe from a particle clump is produced over a period of time of order  $\sim R_B/(\gamma c) \sim 10^{-4} \text{ s}$  in the lab frame. Therefore, the clump acceleration switches to the regime where  $\mathcal{L}_{\perp} \sim R/\gamma$  after a few  $\mu\text{s}$ , and the coherent volume becomes  $V_{coh} \sim \ell_{\parallel}(R/\gamma)^2$ . This leads to the following equation for the clump LF:

$$\gamma \sim \frac{R_B}{R} \left[ \frac{3E(t)}{2qn\ell_{\parallel}} \right]^{1/2} \sim 300 \frac{R_{B,8}}{R_7} \left[ \frac{E_7}{\ell_{\parallel} n_{13}} \right]^{1/2}, \quad (43)$$

which is obtained, as before, by balancing the energy gain and loss rate for particles in the clump. Since the particle density in clumps should be close to the critical density given by equation 9, the above equation can be rewritten as

$$\gamma \sim 800 \left[ \frac{E_7(R)}{\ell_{\parallel} B_9(R)} \right]^{1/2} \frac{[\lambda_{4}^{aw}(R_{ns})]^{1/2} R_{B,8}}{R_7^{1/4}}, \quad (44)$$

where  $E$  and  $B$  are electric and magnetic field perturbation amplitudes associated with the Alfvén wave packet at radius  $R$ . The clump LF has a weak dependence on the radius where the wave becomes charge starved, although it might not seem that way because of the factor  $R_B$  in the numerator. The clump size  $\ell_{\parallel}$  is proportional to plasma length scale ( $\sim c/\omega_p$ ) which is  $\propto R^{3/2}$ , and  $R_B \propto R$ , hence  $R_B/(R^{1/4} \ell_{\parallel}^{1/2})$  is independent of radius, and that means that the clump LF is nearly  $R$ -independent.

An important point to note is that the electric field must be turned on gradually – to be quantified shortly – to ensure that the volume of

the coherent region is large and the clump LF plateaus at  $\sim 10^3$  instead of increasing uncontrollably to  $\gamma \sim 10^8$ , which is the limit when RR force acts on particles individually. The characteristic wavelength of curvature photons at  $t_{rr}$  is given by equation (42). If this wavelength is smaller than  $\sim \ell_{\parallel}$  then the coherent volume decreases as  $\tilde{n}(\pi/\lambda)$  (eq. 33). The smallest clump size is expected to be not much smaller than the plasma length scale according to the two-stream instability (discussed at the beginning of this sub-section). In that case,  $\tilde{n}$  likely decreases exponentially for  $k \gtrsim \ell_{\parallel}^{-1}$ . So, if  $\lambda(t_{rr})$  were to be smaller than  $\ell_{\parallel}$ , then  $\gamma$  would increase with time uncontrollably – an increase of  $\gamma$  produces photons of smaller wavelength and that shrinks the coherent volume, which then reduces RR force causing  $\gamma$  to increase further. The unstable growth of  $\gamma$  is avoided only when  $\lambda(t_{rr}) > \ell_{\parallel}$ , and the electric field turns on slowly such that (see eq. 42)

$$\dot{E} \lesssim (10^{12} \text{ esu s}^{-1}) n_{13}^{\frac{2}{3}} / (R_{B,8} \ell_{\parallel})^{\frac{1}{3}}. \quad (45)$$

As long as the electric field ramps up on the time scale of the Alfvén wave period,  $\sim 10 \mu\text{s}$ , particles within a clump can remain in causal contact while they are being accelerated by the electric field. They are then subjected to the large collective, radiation reaction force, and  $\gamma$  evolves stably. It should be pointed out that clumps moving in the same direction as the Alfvén wave, do not “see” the electric field increase with time since they ride the wave at essentially a fixed phase when their  $\gamma \gtrsim 10^2$ . It follows from the above equation that  $E(t_{rr}) \lesssim 10^4 \text{ esu}$ , since  $t_{rr} \sim 10^{-8} \text{ s}$  (eq. 40).

We have investigated the evolution of particle clump LF for several different parameter regimes. The LF can be related to the effective volume of the region ( $V_{coh}$ ) within which particles suffer the collective RR force. The coherent volume can be considered to be primarily a function of  $\gamma$  for describing the clump dynamics; other parameters, such as plasma density fluctuations and magnetic field curvature radius, are independent of the clump motion to the lowest order. If  $V_{coh}(\gamma)$  were to decline faster than  $\gamma^{-4}$  then the rate of loss of energy per particle, which is proportional to  $p_e N_{coh} \propto \gamma^4 N_{coh}$ , decreases with increasing  $\gamma$ . This is an unstable situation; as  $\gamma$  increases, particles lose less energy and thereby LF goes up. The runaway increase of  $\gamma$  is terminated at a very large value when the electric field energy is depleted or the field shorted by charge redistribution, or the rate of energy loss for an individual particle to curvature radiation is balanced by the rate of work done by the electric field.

We close this sub-section by pointing out the obvious, viz. that the calculations presented here for the Lorentz factor of particle clumps have a higher degree of uncertainty than other parts of the paper. The LF is determined by balancing the electric field acceleration of particles in the clump with the collective radiation reaction force. The latter is not possible to calculate from first principles. We have, instead, relied on energy conservation and causality arguments to provide a rough estimate for the RR force and estimate the clump LF for various possibilities.

### 3 COHERENT CURVATURE RADIATION

Electrons and positrons move in opposite directions along the magnetic field at speed  $\sim c$  below the charge starvation radius,  $R_c$ , to carry the current required by the Alfvén wave-packet. Moreover, electrons and positrons swept up at the head of the Alfvén wave packet at  $R > R_c$  move at different speeds as the electric forces on  $e^+$  and  $e^-$  are in opposite directions. The differential motion between  $e^{\pm}$  is subject to the two-stream instability which leads to formation of clumps as discussed at the beginning of §2.3. The fastest growing modes grow

at a rate  $\omega_p$ , and the longitudinal size of the clumps that form due to 2-stream instability,  $\ell_{\parallel}$ , is of order the plasma length scale,  $\sim \pi c / \omega_p$ , which is given by equation (21).

The curvature radiation produced by electrons moving with LF  $\gamma$ , in a region of transverse size  $\sim R/\gamma$ , adds up coherently<sup>5,6</sup>, since all these electrons have the same acceleration vectors to within an angle  $\gamma^{-1}$  and their velocity vectors are also parallel to within  $\gamma^{-1}$ .

Consider two particles located along the line of sight to the observer and separated by distance  $\delta r$ . These particles are moving with LF  $\gamma$  toward the observer. The relative speed between photons and these particles in lab frame is  $c/2\gamma^2$ . Therefore, the particle in the back should emit a photon before the particle in the front by an amount of time  $\delta t \sim 2\gamma^2 \delta r/c$  (in lab frame) so that these photons arrive at the observer at the same time. If the particle in the front is at a distance  $R$  from the compact object then it has been moving for a time  $\lesssim R/c$  in the lab frame. Since  $\delta t < R/c$ , this construct shows that the largest causally connected radial distance from which photons can arrive at the observer at the same time is  $R/\gamma^2 \equiv \Delta R_{cau}$ .

Particle clumps attain a roughly constant LF  $\sim 10^3$  in a short time of a few  $\mu\text{s}$  as a result of the electric field acceleration and radiation reaction drag force acting collectively on particles in the clump (see §2.3). During the coasting phase, the total number of particles that radiate in phase is (see eqs. 32 & 33)

$$N_{coh} \sim n \ell_{\parallel} (R/\gamma)^2, \quad (46)$$

and the total number of particles from which an observer receives photons at a fixed time is larger than  $N_{coh}$  by a factor  $\sim \Delta R_{cau}/\ell_{\parallel} = R/(\ell_{\parallel} \gamma^2)$ . Making use of equation (22) for curvature power per electron ( $p_e$ ) and equation (46) we obtain the total curvature power to be

$$P_c = N_{coh}^2 (\Delta R_{cau}/\ell_{\parallel}) p_e = \frac{2q^2 c R^5 \ell_{\parallel} n^2}{3R_B^2 \gamma^2}. \quad (47)$$

The luminosity in the observer frame is

$$L_{iso} \approx 8\gamma^4 P_c \approx \frac{16q^2 c R^5 \gamma^2 n^2 \ell_{\parallel}}{3R_B^2}. \quad (48)$$

We can use equation (23) to replace  $\gamma$  in favor of  $\nu$  and express the FRB luminosity in a more convenient form

$$L_{iso} \approx \frac{16(2\pi)^{2/3} q^2 c^{1/3} R^5 n^2 \ell_{\parallel} \nu^{2/3}}{3R_B^{4/3}}. \quad (49)$$

Replacing  $\ell_{\parallel}$  using equation (21), and  $n \approx n_c$  (eq. 9 gives  $n_c$ ), leads to the following expression for the luminosity

$$L_{iso} \approx (10^{44} \text{ erg s}^{-1}) \left[ \frac{B_{11}}{\lambda_{4}^{aw\perp}} \right]^{\frac{3}{2}} \frac{\nu_9^{\frac{2}{3}}}{R_{B,8}^{\frac{4}{3}}} \left[ \frac{R_c}{R} \right] \left[ \frac{R_c}{10R_{ns}} \right]^{\frac{1}{2}}, \quad (50)$$

where  $R_c$  is the charge starvation radius,  $R$  is the radius where curvature radiation is produced (which should be the same as  $R_c$  or very close to it),  $\lambda^{aw\perp} \equiv 2\pi/k^{aw\perp}$ ,  $k^{aw\perp}$  is the transverse component of Alfvén wave-vector and  $B$  is Alfvén wave amplitude, both of which

<sup>5</sup> The angle between magnetic field lines, for a dipole magnet, at two locations at the same radius but separated by an angle  $\delta\theta$  can be shown to be  $3\delta\theta(1 + \cos^2\theta)/(1 + 3\cos^2\theta)$  which is  $3\delta\theta/2$  near the pole, and  $3\delta\theta$  at the equator.

<sup>6</sup> Consider two photons produced at the same time in the lab frame via the curvature radiation mechanism. One of these photons is emitted by an electron located at  $(R, \theta = 0)$  and the other one at  $(R+R/2\gamma^2, \theta = \gamma^{-1})$  arrive at the observer at the same time. The magnetic field directions at these two locations are within an angle  $\gamma^{-1}$  and so are the velocity and acceleration vectors of particles at these places. Therefore, both these photons arrive at the observer at the same time with the same phase angle, and hence add up coherently.

are evaluated at the wave launching site, i.e. at the NS surface;  $k^{aw\perp}$  is larger than  $k^{aw\parallel} = \omega_{aw}/c$  at the surface of the NS by a factor  $\sim 10$ – $10^2$ . The magnetic field produced by the motion of charge clumps must be smaller than the original field by at least a factor  $\gamma$  in order to maintain coherent addition of radiation from different particles in the clump (Kumar et al. 2017). This condition is satisfied at  $R_c$  provided that the magnetic field strength at the NS surface is  $\gtrsim 10^{14}$  G.

The specific luminosity  $L_{iso}^\nu \sim L_{iso}/\nu \propto \nu^{-1/3}$ . The dependence of luminosity on frequency is more complicated than suggested by this equation;  $L_{iso}^\nu$  depends on the distribution of clump sizes and their LFs. In terms of the Fourier transform of particle number density  $n(\mathbf{x})$ , i.e.  $\tilde{n}(k)$ ,  $L_{iso}^\nu \propto \nu^{2/3} |\tilde{n}(k)|^2$  in the high frequency limit of  $\nu \gtrsim c/\ell_{\parallel}$  (see eq. 33); where  $|k| = 2\pi\nu/c$ .

If the minimum clump size is the plasma length scale or  $\sim \ell_{\parallel}$ , as suggested by the two-stream instability, then  $|\tilde{n}(k)|$  falls off exponentially for  $\nu \gtrsim c/\ell_{\parallel}$  ( $\ell_{\parallel}$  is given by eq. 21). Therefore, the luminosity is expected fall off sharply at  $\nu \gtrsim c/\ell_{\parallel}$ .

The electric field develops before the Alfvén wave reaches the charge starvation radius  $R_c$  as the plasma is clumpy due to 2-stream instability and possibly other effects. However, the field strength at  $R < R_c$  is smaller than  $E_d$  (eq. 7), which is the value of the electric field in the fully charge starved region. Let us take the field strength in the transition zone to be  $\eta E_d$ ;  $\eta$  is a function of radius  $R$ . The electric force is balanced by the radiation reaction force acting collectively on particles in the clump as discussed in §2.3. In this case, the rate of energy radiated per unit volume is equal to the work done by the electric field  $E$ , i.e.

$$\epsilon_{em} = qnc\eta E_d \sim qnc\eta B(k_{aw\perp}/k_{aw\parallel}). \quad (51)$$

The energy density in Alfvén waves is  $B^2/4\pi$ , and therefore the dissipation length for the wave is

$$d_{aw} = \frac{cB^2}{4\pi\epsilon_{em}} \sim \frac{B}{4\pi qn\eta} \left[ \frac{k_{aw\parallel}}{k_{aw\perp}} \right] \sim 2 \times 10^5 \text{ cm} \frac{B_{10}(R)}{\eta n_{13}}, \quad (52)$$

where  $B/n \propto R^{3/2}$  is calculated at the charge starvation radius. The Alfvén wave damps rapidly as it approaches the charge starvation radius; the dissipation length is roughly of order  $\eta^{-1}$  times the wavelength of the waves, and the wave loses a large fraction of its energy in the vicinity of  $R_c$ .

### 3.1 Predictions of the model

#### • Maximum frequency for FRBs

The EM spectrum is cutoff exponentially for wavelengths much smaller than particle clump size or the longitudinal size of the coherent region. We find the cutoff frequency using equation (21):

$$\nu_{max} \sim c/\ell_{\parallel} \sim 50 \text{ GHz} \left[ \frac{B_{11}(R_{ns})}{\lambda_4^{aw\perp}(R_{ns})} \right]^{1/2} \left[ \frac{10R_{ns}}{R_c} \right]^{3/2}. \quad (53)$$

This assumes that clumps have a distribution of  $\gamma$ , which they do when the ratio of the electric field strength (the component parallel to the static magnetic field) and the wave-magnetic field ( $E/B$ ) fluctuates, perhaps as a result of large density variation near the charge starvation region (eqs. 43 & 44). The  $\gamma$ -distribution can only be determined by a very demanding numerical simulations of Alfvén waves in charge starvation region that includes the 2-stream instability. Coherent radiation at a frequency much larger than 50 GHz can be produced only if plasma density fluctuations were to extend well below the plasma length scale ( $\sim c/\omega_p$ ), which is unlikely but cannot be ruled out

$$\nu \propto \gamma^3/R_B \propto \ell_{\parallel}^{-3/2} (R_B^2/R) (E/B)^{3/2} \lambda_{aw\perp}^{3/2} \quad (54)$$

#### • Minimum frequency for FRBs

The maximum wavelength of radiation for particle clumps moving with LF  $\gamma$  is given by the radial size of causally connected region, i.e.  $R/2\gamma^2$ , which is larger than the typical  $\lambda$  of radiation from these bunches by a factor  $\gamma R/(2\pi R_B) \sim 20 \gamma_3 R_7/R_{B,8}$ ;  $R$  is the radius at which radiation is produced and  $R_B$  is the radius of curvature of magnetic field lines there. Equating the curvature radiation wavelength ( $2\pi R_B/\gamma^3$ ) with  $R/2\gamma^2$ , we find the LF of clumps which produce radiation of characteristic wavelength the size of causally connected region

$$\gamma \sim \frac{4\pi R_B}{R_c} \implies \lambda_{max} \sim \frac{2\pi R_B}{\gamma^3} \sim 300 \text{ cm} \frac{R_{c,7}^3}{R_{B,8}^2}; \quad (55)$$

where  $R_c$ , as before, is the charge starvation radius for the Alfvén wave where the FRB radiation is produced, and  $R_B$  is the radius of curvature of magnetic field lines in the radiation region at  $R_c$ . So, the minimum frequency of radiation according to the model is  $\nu_{min} \sim 10^2 \text{ MHz} R_{B,8}^2/R_7^3$ . The size of clumps which have the appropriate LF for producing  $\nu_{min}$  can be obtained from equation (43) and is given by  $\sim 40 \text{ cm} R_7^{3/2} E_7 \lambda_4^{aw\perp}/B_9(R)$ .

The transverse size of the region from which an observer receives photons is the smaller of the length scales  $\sim R/\gamma \propto R/\nu^{1/3}$  and the transverse size of the Alfvén wave-packet where the radiation is produced ( $w_{aw\perp}$ ). If  $w_{aw\perp} < 2\lambda_{max}\gamma$  then the observed luminosity declines as  $\nu^{4/3}$  at low frequencies modulo the power spectrum of fluctuations in  $\gamma$  on the corresponding length scale.

The discussion, thus far, has been about the intrinsic source properties. However, as the radiation propagates through the circumstellar medium, it is subjected to strong induced-Compton scatterings and loss of energy as particles along its path are accelerated to large Lorentz factors out to distances of  $\sim 10^{14}$  cm of the source (Kumar and Lu, 2019). The magnitude of these propagation effects increases with decreasing photon frequency roughly as  $L_\nu/\nu^2$ , which can become substantial at  $\lambda_{min}$  depending on the unknown properties of the CSM of FRBs.

#### • Minimum & maximum luminosities for FRBs

Low luminosity Alfvén waves might never become charge starved, and hence, according to the model presented here, there should be a minimum floor for the FRB luminosities. The absolute minimum is set by the consideration that the charge starvation density ( $n_c$ ) is equal to the Goldreich-Julian density ( $n_{G,J}$ ). Since plasma density in NS magnetosphere is  $\gtrsim n_{G,J}$ , when  $n_c < n_{G,J}$  the Alfvén wave packet can travel without becoming charge starved to large distances from NS surface. Therefore, particles clumps don't get accelerated to produce coherent radiation. The condition that  $n_c \gtrsim n_{G,J}$  implies that the Alfvén wave amplitude  $B(R_{ns}) \gtrsim 7 \times 10^8 B_{ns,15} \lambda_4^{aw\perp}/P_{ns}$  Gauss (eqs. 9 & 10); where  $B_{ns}$  is NS surface magnetic field,  $P_{ns}$  is its rotation period, and  $\lambda^{aw\perp}$  is the transverse cross-section of the Alfvén wave packet at the wave launching radius. Thus, the Alfvén wave luminosity at the NS surface, before correcting for the finite beam angle, is  $L_{aw} \sim 10^{36} [B_{ns,15} \lambda_4^{aw\perp}]^2 / P_{ns}^2 \text{ erg s}^{-1}$ . The isotropic luminosity of the wave at the radius where it becomes charge starved and produces FRB radiation is  $L_{iso}^{aw}(R_c) \sim B(R_{ns})^2 [R_{ns}/R_c]^3 R_c^2 \sim 10^{39} [B_{ns,15} \lambda_4^{aw\perp}]^2 / (R_{c,7} P_{ns}^2) \text{ erg s}^{-1}$ . The efficiency for converting Alfvén wave luminosity to FRB radiation is very high as discussed below equation (52), therefore, the minimum FRB luminosity is

$$L_{FRB}^{min} \sim 10^{39} \text{ erg s}^{-1} \frac{[B_{ns,15} \lambda_4^{aw\perp}]^2}{R_{c,7} P_{ns}^2}. \quad (56)$$

The  $L_{FRB}^{min}$  calculated above is for an observer whose line of light lies within the relativistic cone of the source. The bolometric luminosity outside the relativistic beam falls off rapidly with increasing angle ( $\theta$ ) from the edge of the cone as  $(\theta\gamma)^{-6}$ , and the peak of the spectrum shifts to lower frequencies as  $(\theta\gamma)^{-2}$ .

The maximum luminosity for FRBs is estimated to be  $\sim 10^{49} R_{B,8}^2 B_{n_s,15} \text{ erg s}^{-1}$  as discussed in Lu and Kumar (2019).

#### • Beaming angle and true energy

There are three different angular scales in the system. The first one is the angular size of the region about the magnetic pole from which FRB producing Alfvén waves are launched ( $\theta_{aw}$ ). The other two are the relativistic beaming, and the angular size of the FRB source.

In order for an Alfvén wave packet to produce an FRB, it should be able to travel to large enough distances from the neutron star surface where it becomes charge starved. A magnetic field line emerging from the NS surface at polar angle  $\theta$  wrt to the magnetic pole reaches a maximum distance of  $R_{n_s}/\sin^2\theta$  and then curves back toward the NS surface. Hence, Alfvén waves that originate within an angle  $\theta_{aw} \lesssim 0.2$  rad of the magnetic pole can travel out to a few 10s of  $R_{n_s}$ , and have a greater chance of running into a low density plasma, become charge starved, and produce a FRB.

The LF of particle clumps that produce GHz photons via curvature radiation is of order  $10^3$  (eq. 23), and these photons are beamed in a cone of opening angle  $\sim 10^{-3}$  rad. However, a burst is observable over a much larger fraction of the sky, which is the angular size of Alfvén wave packet at the radius where the coherent radiation is produced. Alfvén wave packets move along diverging dipole magnetic field lines and their transverse size increases with radius as  $\lambda^{aw\perp}(R_{n_s})[R/R_{n_s}]^{3/2}$ . Thus, the angular size of the wave packet at radius  $R$  is

$$\theta_{frb} \sim \frac{\lambda^{aw\perp}(R_{n_s})}{R_{n_s}} \left[ \frac{R}{R_{n_s}} \right]^{\frac{1}{2}} \sim 2 \times 10^{-2} \text{ rad } \lambda_{4,4}^{aw\perp} R_7^{\frac{1}{2}}. \quad (57)$$

The total energy associated with a FRB event that has isotropic luminosity  $10^{44} \text{ erg s}^{-1}$  and duration 1 ms, after correcting for the beaming, is

$$E_{frb} \sim \frac{L_{frb} t_{frb} \theta_{frb}^2}{4} \sim 10^{37} \text{ erg } R_7 [\lambda_{4,4}^{aw\perp}(R_{n_s})]^2. \quad (58)$$

The probability of seeing a burst from a random magnetar is  $\theta_{frb}^2/4 \sim 10^{-4}$ . If a magnetar produces a larger number of bursts, we expect them all to be within a solid angle  $\pi\theta_{aw}^2(R/R_{n_s})$  based on the above argument<sup>7</sup>. So the probability for a random observer to see one of these large number of bursts is  $\theta_{aw}^2(R/R_{n_s})/4 \lesssim 10\%$ . The probability for an FRB from one of the  $\sim 30$  magnetars in our galaxy might be considerably smaller if the FRB activity is associated with young magnetars; magnetars in our Galaxy are  $\gtrsim 10^3$  years old (Tendulkar, 2014).

#### • Periodicity of repeated bursts from an object?

According to our model, only those Alfvén waves that are launched from the NS surface within a distance  $\theta_{aw}R_{n_s}$  of the magnetic pole can travel out to a distance of a few 10s of NS radii, where they become charge starved and produce FRBs;  $\theta_{aw} \sim 0.2$  as discussed under the previous bullet point. The angular size of an Alfvén wave packet moving along magnetic field lines increases with radius as  $R^{1/2}$ . Thus, we expect coherent radio waves to be produced within

<sup>7</sup> The fraction of the sky where one of the bursts from the object can be seen is larger than  $\pi\theta_{aw}^2(R/R_{n_s})$  if the angle between the magnetic and rotation axis is  $\gtrsim \theta_{aw}(R_c/R_{n_s})^{1/2} \sim 1$  rad. This is because, in this case, the sweep of the rotation axis enlarges the solid angle coverage of Alfvén wave packets.

a cone of angular size  $\theta_{aw}(R_c) \sim \theta_{aw}(R_c/R_{n_s})^{1/2} \sim 1$  rad, around the magnetic axis, and occurring almost randomly in time. If the angle between the rotation and the magnetic axis is much smaller than  $\theta_{aw}(R_c)$  then there is no preferred phase of the NS rotation when we see bursts. However, if the inclination between the two axis is of order  $\theta_{aw}(R_c)$ , or larger, then we would only see bursts from an object during a limited NS rotation phase when the Alfvén cone is pointing at us. This effect is somewhat more pronounced for stronger bursts, which are produced by Alfvén waves of higher luminosity, which become charge starved at a smaller radius and have smaller  $\theta_{aw}(R_c)$ . This is something that observers can investigate when we have data for a large number of bursts from an object such as FRB 121102.

## 4 DISCUSSION

We have described a model for FRBs where large amplitude Alfvén waves are produced by some disturbance at the surface of a magnetar in the magnetic pole region, and as these waves travel to larger radii they decay and produce coherent radiation (Fig. 1 shows the main components of the model). Alfvén wave packets require a non-zero current along the static magnetic field as long as the transverse component of their wave-vector is non-zero. The current becomes stronger as the wave travels to larger radii. The counter-streaming  $e^{\pm}$ s that carry the current are subject to the two two-stream instability, which leads to formation of particle bunches of size of order the plasma scale. At some large radius, of order a  $10 R_{n_s}$ ,  $e^{\pm}$  density is insufficient to supply the current the wave packet requires. This is the region of charge starvation for the Alfvén wave. Strong electric field develops along the magnetic field in the charge starvation region, which provides the displacement current to make up for the deficit in  $e^{\pm}$  current. The electric field sweeps up particles and accelerates them to different speeds depending on their charges. The resulting differential motion also leads to clump formation. Particle bunches are accelerated by the electric field to LF  $\sim 10^3$ . They follow the curved magnetic field lines and produce the powerful coherent FRB radiation.

The Alfvén wave luminosity at the launching site is  $B^2 c \lambda_{aw\perp}^2 / 4\pi$ ; where  $\lambda_{aw\perp}$  is the transverse size of the wave packet. The transverse size of the wave packet increases with radius as  $R^{3/2}$  as the wave follows the diverging dipole magnetic field lines of the magnetar. Thus, the wave packet cross-section area at the radius  $R$  where the radiation is produced is  $\lambda_{aw\perp}^2(R/R_{n_s})^3$ , and the angular size of the beam over which the radiation is spread is  $(\lambda_{aw\perp}/R_{n_s})(R/R_{n_s})^{1/2}$ . The efficiency for conversion of Alfvén wave luminosity to radio waves is very high in our model. Hence, the isotropic equivalent of the emergent FRB luminosity is  $B(R_{n_s})^2 R_{n_s}^3 c / R$ , and to produce a FRB of luminosity  $10^{44} \text{ erg s}^{-1}$  Alfvén waves with amplitude  $B(R_{n_s}) \sim 10^{11} \text{ G}$  are required.

An Alfvén wave packet of amplitude  $B(R_{n_s}) \sim 10^{11} \text{ G}$  becomes charge starved when  $e^{\pm}$  density of the medium at radius  $R$  falls below  $\sim 10^{13} / R_7^3 \text{ cm}^{-3}$ . The plasma frequency in the charge starvation region is estimated to be  $\sim 30 R_7^{-3/2} \text{ GHz}$ , and clumps that form due to two-stream instability have radial width  $\sim (1 \text{ cm}) R_7^{3/2}$ .

Calculations of electric field in the charge starvation region, the formation and acceleration of  $e^{\pm}$  clumps are presented in §2.1 and 2.3. Acceleration of clumps which are subjected to collective radiation reaction forces – because particles in the clump radiate in phase – is a problem that cannot be solved from first principles. We have relied on causality and energy conservation arguments to model radiation reaction forces and estimate clump Lorentz factor in the electric field of Alfvén waves in charge starvation regions. We find that

clumps are accelerated by the intense electric field on a time scale of  $\sim 10$  ns to Lorentz factor  $\sim 10^3$ . Particles with this LF produce curvature radiation at a frequency of  $\sim 1$  GHz. The observed frequencies and luminosities of FRBs can be understood if Alfvén waves become charge starved somewhere between a few times  $R_{ns}$  and  $\sim 10^2 R_{ns}$ .

The predictions of the model are described in §3. We find that the minimum and the maximum frequencies expected for FRBs according to this model are  $\sim 100$  MHz and  $\sim 10^2$  GHz respectively. The minimum FRB luminosity (isotropic equivalent) is  $\sim 10^{39} [B_{ns,15} \lambda_{4}^{aw}]^2 / (R_7 P_{ns}^2)$  erg  $s^{-1}$ , which is set by the fact that lower luminosity Alfvén waves don't become charge starved as they travel through the magnetosphere, and hence they don't decay and produce coherent EM waves. The beaming angle of FRBs, according to this model, is about  $10^{-2}$  rad, and thus the total energy budget of a typical fast radio burst is of order  $10^{36}$  erg. These predictions are dependent on a few uncertain parameters, the primary one of which is the radius where the Alfvén wave becomes charge starved. These dependencies can be found in appropriate equations in §3.

## 5 ACKNOWLEDGMENTS

We thank the referee for numerous helpful comments and suggestions, which clarified many concepts and improved the paper. PK would like to thank Bing Zhang and Wenbin Lu for comments and discussions.

## REFERENCES

- Bannister, K.W. et al. 2017, ApJL 841, L12  
 Bannister, K.W. et al. 2019, Science 365, 565  
 Beloborodov, A.M. 2017, ApJ 843, L26  
 Blaes, O., Blandford, R.D., Goldreich, P., Madau, P. 1989, ApJ 343, 839  
 Chen, F.F., 1974, Introduction to Plasma Physics, Springer  
 CHIME/FRB Collaboration, Amiri, M. et al. 2019a, Nature 566, 230  
 CHIME/FRB Collaboration, Amiri, M., et al. 2019b, Natur 566, 235  
 Chatterjee, S. et al. 2017, Nature 541, 58  
 Cordes, J. M., Wasserman, I., Hessels, J. W. T., Lazio, T.J.W., Chatterjee, S., and Wharton, R.S. 2017, ApJ, 842, 35  
 Dirac, P. A. M., 1938, Proceedings of the Royal Society of London, Series A, 167, 148  
 Farah et al. 2018, MNRAS 478, 1209  
 Gajjar, V. et al. 2018, ApJ 863, 2  
 Ghisellini, G. & Locatelli, N. 2018, AA 613, 61  
 Goldreich, P. and Julian, W.H. 1969, ApJ 157, 869  
 Hessels, J.W.T. et al. 2019, ApJ 876, L23  
 Katz, J. I. 2014, Phys. Rev. D, 89, 103009  
 Katz, J. I. 2016, ApJ 826, 226  
 Katz, J.I. 2018, Progress in Particle and Nuclear Physics 103, 1  
 Kulsrud, R. M. 2005, *Plasma Physics for Astrophysics*, Princeton University Press, Princeton & Oxford  
 Kumar, P., Lu, W. and Bhattacharya, M. 2017, MNRAS 468, 2726  
 Kumar, P., Lu, W. 2019, submitted to MNRAS  
 Landau, L. & Lifshitz, E. 1971, The Classical Theory of Fields, Pergamon Press  
 Law, C.J. et al., 2017, ApJ 850, 76  
 Lorimer, D.R., Bailes, M., McLaughlin, M.A., Narkevic, D.J., Crawford, F., 2007, Science 318, 777  
 Lu, W. and Kumar, P. 2018, MNRAS 477, 2470  
 Lu, W. and Kumar, P. 2019, MNRAS 483, L93  
 Marcote, B. et al. 2017, ApJ 834, L8  
 Metzger, B.D., Berger, E., and Margalit, B. 2017, ApJ 841, 14  
 Metzger, B.D., Margalit, B., and Sironi, L. 2019, MNRAS 485, 4091  
 Michilli, D. et al., 2018, Nature 553, 182  
 Murase, K., Kashiyama, K., Meszaros, P., 2016, MNRAS 461, 1498  
 Murase, K., Meszaros, P., Fox, D.B., 2017, ApJL 836, L6  
 Osłowski, S. et al. 2019, MNRAS 488, 868  
 Petroff, E., Barr, E.D., Jameson, A., Keane, E.F., Bailes, M., Kramer, M., Morello, V., Tabbara, D. and van Straten, W., 2016, Pub. Astro. Soc. of Australia, 33, e045  
 Ravi, V. 2019a, MNRAS 482, 1966  
 Ravi, V. 2019b, [arXiv:1907.06619](https://arxiv.org/abs/1907.06619)  
 Ravi, V. et al. 2019, Nature, [arXiv:1907.01542](https://arxiv.org/abs/1907.01542)  
 Shannon, R.M. et al. 2018, Nature 562, 386  
 Spitler, L.G. et al. 2014, ApJ 790, 101  
 Spitler, L.G. et al. 2016, Nature 531, 202  
 Tendulkar, S.P. et al. 2017, ApJ 834, L7  
 Tendulkar, S.P. 2014, Ph.D. Thesis Caltech  
 Thompson, C. 2019, ApJ 874, 48  
 Thornton, D. et al. 2013, Science 341, 53  
 Wang, W., Zhang, B., Chen, X., and Xu, R. 2019, ApJ. 876, L15  
 Wang, J-S & Lai, D. 2019, [arXiv:1907.12473](https://arxiv.org/abs/1907.12473)  
 Weinberg, S. 1962, Phy. Rev. 126, 1899  
 Zhang, B. 2017, ApJ 836, L32